Two-dimensional imaging of a second-order nonlinear optical process

Indrajit Bhattacharyya and Debabrata Goswami*

Department of Chemistry, Indian Institute of Technology, Kanpur 208 016, India

Spatiotemporal imaging of sum-frequency generation process through second-order nonlinear optical interaction in a nonlinear crystal under femtosecond pulsed illumination is presented. Two focal points in the spatial dimension that result from use of widely separated wavelengths (780 and 1560 nm) including their appropriate intensity ratios are captured accurately, emphasizing the sensitivity and robustness of this detection scheme. Most importantly, cross-correlation width that is used as characteristic measure from such techniques remains constant at the two focal points. However, this highlights the critical role of nonlinear crystal position along beam propagation axis during such collinear intensity cross-correlation measurements involving different wavelengths.

Keywords: Nonlinear optics, nonlinear optical signal processing, nonlinear optical materials, ultrafast lasers.

SECOND-order nonlinear optical (NLO) processes in crystals[1], such as second-harmonic generation (SHG), sum frequency generation (SFG) or optical parametric amplification, are useful and popular techniques to produce and characterize ultrashort laser pulses in different spectral regimes. Generation of SFG signal through interaction of two short laser pulses in a nonlinear BBO (β-barium borate, β-BaB_2O_4)[2–4] crystal commonly involves non-collinear beam geometry, where two laser beams propagate at an angle inside the crystal; however, collinear beam geometry can also be used, depending on the motivation and scheme of the experiment[5–8]. Unlike non-collinear cross-correlation scheme, correlating pulses in the collinear setup interact over a longer propagation distance inside the crystal resulting in lower threshold and more efficient SFG[7]. Thus collinear geometry is often utilized for characterization of ultrashort pulses in multiphoton microscopy. Collinear mode provides the tightest focus, best spectral and temporal intensity, finest spectral resolution and the best possible elimination of temporal blurring[5]. These are crucial for optimization of laser pulses at the sample plane of nonlinear microscope, which in turn, maximizes the generated nonlinear signal on biological samples while minimizing radiation dosage resulting in increased specimen lifetime[7].

Here, we use a collinear Mach-Zehnder type interferometric set-up to record a spatiotemporal image of SFG cross-correlation signal at 520 nm, resulting from the interaction of two short laser pulses at 1560 and 780 nm inside a BBO crystal. The nonlinear crystal is translated along the direction of laser beam propagation (Z-axis) and the corresponding temporal correlations at every Z position of the BBO crystal are recorded. The main focus of the present study is to explore features of spatiotemporal image of second order NLO process by mapping SFG intensities in two different dimensions: one is the time delay between cross-correlating pulses (time profile) and the other is the axis along which BBO crystal is translated across the focal points (Z-axis) of the combined cross-correlating beams (spatial profile). Use of single lens to focus input pulses inside the BBO crystal results in two foci due to wavelength dependence, which are precisely resolved and accurately captured with appropriate intensity ratio on the Z axis. Furthermore, we find that the shortest possible temporal correlation is only possible at the two focal points, which highlights the spatiotemporal significance of the present work.

We use an Er : doped mode-locked femtosecond fibre laser (Femtolite C-20-SP, IMRA Inc.), which generates 50 MHz collinear laser pulses, centred at the fundamental wavelength 1560 nm and its second harmonic 780 nm as a single output (Figure 1). The 1560 nm pulse is ~300 fs wide and has a 40 mW average power, while the 780 nm pulse is ~100 fs wide with a 20 mW average power. A collinear cross-correlation set-up is built based on Mach-Zehnder geometry, where two dichroic beam splitters are used: the first one separates the two wavelengths, while the second one recombines them.

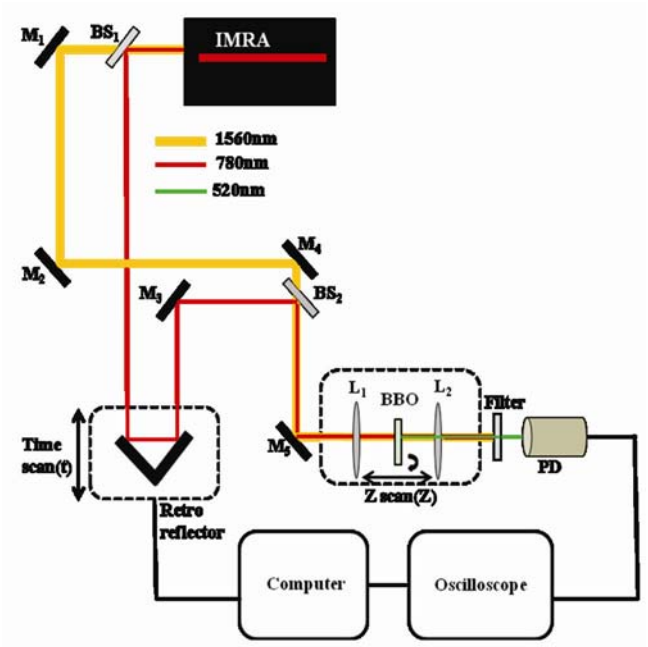

Figure 1. Schematic of the experimental set-up. The inset describes the focal point geometry after the first focusing lens. BS, beam splitter; M, mirror; L, lens.

*For correspondence. (e-mail: dgoswami@iitk.ac.in)

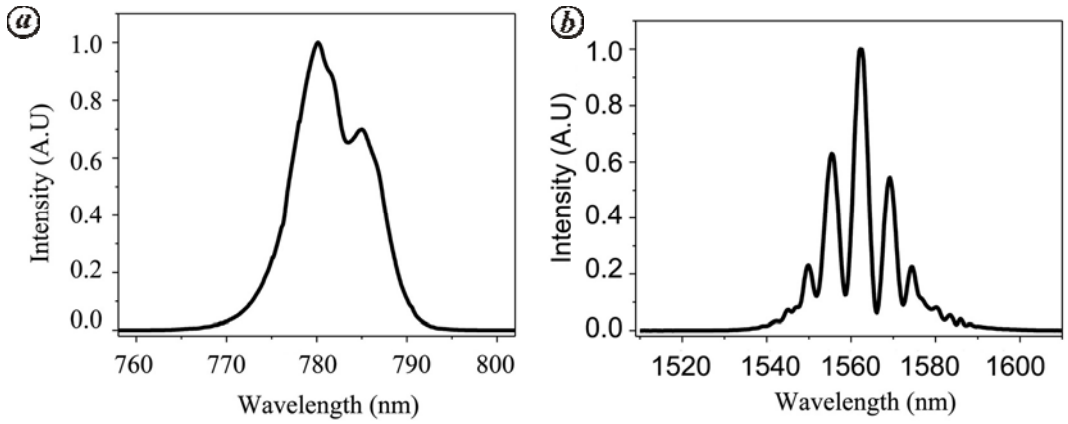

Figure 2. Spectra of (***a***) 780 nm and (***b***) 1560 nm pulse coming out directly from the laser.

The recombined laser pulses, after the second dichroic mirror, are focused into a type-I BBO (β-barium-borate) nonlinear crystal (0.5 mm) by a single BK7 lens (L_1, $f = 50$ mm) to generate cross-correlation signal at 520 nm. The 520 nm signal is filtered using a 780 nm NIR-cut short-pass filter and is collected by a second lens (L_2) focusing onto a silicon photodiode (PD) detector as a function of time-delay between the correlating pulses (Figure 1). This is measured with a 500 MHz oscilloscope (LeCroy LT354M) interfaced to the computer with a National Instruments GPIB card. In order to determine the time zero ($t = 0$) by matching the path lengths between the two cross-correlating laser pulses, a retro-reflector is used in the 780 nm beam path on a motorized translation stage (model ESP-300), which can step with a minimum resolution of 0.055 μm (0.37 fs). An additional translation stage stepping with a minimum resolution of 0.017 μm has been used to move the BBO across the focal point of the first lens (L_1). Cross-correlation traces are acquired at every Z-position in the BBO crystal as it is scanned along the direction of the beam propagation (Z-axis) around the focus. The resulting cross-correlation intensities have been plotted with respect to both the time and the Z-axis to generate a two-dimensional image of the second-order NLO signal. All data acquisition is performed using LabVIEW programing and subsequent analysis is done using Origin and MATLAB.

SFG through intensity cross-correlation is a second-order nonlinear process, where the intensity of the generated cross-correlation signal (in our particular case 520 nm resulting from the cross-correlation of 1560 nm and 780 nm) can be expressed mathematically as

$$I_{520}(\tau) = \int_{-\infty}^{\infty} |E_{1560}(t)E_{780}(t-\tau)|^2 \mathrm{d}t$$

$$= \int_{-\infty}^{\infty} I_{1560}(t)I_{780}(t-\tau)\,\mathrm{d}t, \quad (1)$$

where $I_{520}(\tau)$ is the intensity of the cross-correlation signal at 520 nm. $|E_{1560}(t)|$ and $|E_{780}(t-\tau)|$ are the electric fields corresponding to 1560 nm and time delayed 780 nm pulses respectively. $I_{1560}(t)$ and $I_{780}(t-\tau)$ are respective intensities of 1560 nm and time delayed 780 nm pulses. The 780 nm pulses emerging from IMRA laser have relatively simple pulse shapes (Figure 2 *a*), whereas pulses centred at 1560 nm show a more complex nature with comb-like spectral features over a larger bandwidth (Figure 2 *b*). The effect of exact spectral features is within errors of our experimental measurements.

We record the spatiotemporal intensity profile of the collinear SFG cross-correlation signal generated by 1560 and 780 nm pulses into a 0.5 mm thin BBO crystal by combining the conventional time scans with Z-scan of the BBO across the focal points of the combined pulses after the second dichroic mirror. In conventional single beam Z-scan experiments[9,10], position and intensity-dependent transmission from the sample are measured by moving the sample across the focal point of the lens along the Z-axis. This measures the nonlinear absorption and nonlinear refraction of the sample at a particular wavelength. In our experiments, instead of measuring the effect of a single beam, we use two collinear laser beams interacting inside the BBO crystal and measure only the intensity of the SFG signal, resulting from the phase matching interaction of the individual laser pulses while moving the crystal across the focal point of L_1 along the Z-axis at each time delay between the two pulses (Figure 3).

Initially, the cross-correlation signal is optimized for the maximum temporal and spatial overlap between the laser pulses (i.e. $t = 0$, $Z = 0$, Figure 4 *a* and *b* respectively) and then the position of the BBO crystal is changed across $Z = 0$ and correspondingly the cross-correlation trace at each individual Z-position is recorded.

Figure 5 shows the two-dimensional intensity map of the cross-correlation signal at 520 nm, where the SFG cross-correlation intensities are plotted with respect to both the delay on time axis and individual Z positions of

the BBO crystal along the Z axis. Since the interacting wavelengths in our case, 1560 and 780 nm, are widely separated, it was not possible to find a suitable achromatic lens for focusing the two cross-correlating beams at the same point inside the BBO crystal. Instead, a non-achromatic lens was used in the present experiment, which makes the beams focused at two different points separated by a finite gap on the Z-axis (Figure 3). Consequently, two different maxima appear in the Z-scan trace of the BBO as observed in Figures 4 *b* and 5.

Focal length being a function of wavelength, calculation of focal lengths corresponding to two different wavelengths (1560 and 780 nm for our case) with respect to a particular non-achromatic bi-convex lens and the separation between them is possible by using Lens-making formula, which is expressed as

$$\frac{1}{f_\lambda} = (n_\lambda - 1)\left[\frac{2}{R} - \frac{(n_\lambda - 1)}{n_\lambda R^2} d\right], \tag{2}$$

where f_λ and n_λ are the actual focal length and the refractive index of the lens material respectively, for wavelength λ, R the radius of curvature and d is the centre thickness of the lens. In our experiment, we use a 50 mm BK-7 glass biconvex lens to focus both the laser beams at the BBO crystal. The respective refractive indices corresponding to 1560 and 780 nm are 1.5 and 1.511. The radius of curvature and the central thickness of the lens are 5.2 and 50.6 mm respectively. Calculation using the above equation shows that the actual focal lengths of the lens should be 52.6 and 50.5 mm respectively, for 1560 and 780 nm, indicating that 780 nm beam gets focused to its minimal spot size position ~2 mm ahead of the focal point of 1560 nm (Figure 3). Thus we can explain the origin of the two maxima and their separation of 2 mm under the present experimental condition as seen from Figures 4 *b* and 5.

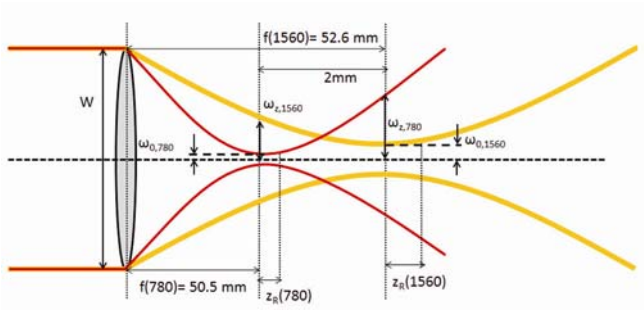

Figure 3. Details of beam geometry and beam parameters as used in the present experiment. W is the Gaussian beam waist for both the laser beams as they are coming through an identical beam aperture; f(780) and f(1560) are focal lengths of the non-achromatic lens with respect to 780 and 1560 nm respectively; $\omega_{0,780}$ and $\omega_{0,1560}$ are respective beam waist radii for 780 and 1560 nm beam at the focal points; z_R(780) and z_R(1560) are the Rayleigh ranges of 780 and 1560 nm beam respectively; $\omega_{z,780}$ and $\omega_{z,1560}$ are the respective beam waists radii of 780 and 1560 nm beam at the focal points of 1560 and 780 nm respectively.

The initial Gaussian beam waist of both the laser beams is experimentally found to be 2.77 mm as they come through an identical beam aperture. The experimental measurement involved recording the residual intensity while a knife edge was translated across either of the laser beams. The measured signal was integrated in both cases to result in Gaussian profiles, whose FWHM provided laser beam-waist values[11,12].

In order to explain the intensity ratio of SFG signals originating at Z = 0 mm and Z = 2 mm, we calculated the total effective intensities of 780 and 1560 nm beam at each of the two wavelength-dependent focal spots, which are proportional to the overall intensities of the generated SFG signals at these two points. This particular calculation is based on Gaussian optics approximations, where the beam waists (ω_0) of 780 nm ($\omega_{0,780}$ = 9.05 μm) and 1560 nm ($\omega_{0,1560}$ = 18.85 μm) at their respective focal points are calculated as

$$\omega_0 = 2\lambda f / \pi W, \tag{3}$$

where ω_0 is the beam waist at the focal point, λ the wavelength, f the focal length and W is the initial beam waist before the focusing lens.

At the focal point of 780 nm beam, we calculated the peak intensity of 780 nm (I_{780}) as

$$I_{780} = P_{780} / \pi\omega_{0,780}^2, \tag{4}$$

where P_{780} is the peak power of 780 nm beam at the beam waist of 780 nm and $\omega_{0,780}$ is the beam waist of 780 nm beam at the focal point of 780 nm. At the same point, we calculate the effective peak intensity of 1560 nm (I_{1560}) beam as

$$I_{1560} = \frac{P_{1560}}{\pi\omega_{z,1560}^2} \times \left[\frac{\omega_{0,1560}}{\omega_{z,1560}}\right]^2 \times \exp\left[-2\left(\frac{\omega_{0,780}}{\omega_{z,1560}}\right)^2\right], \tag{5}$$

where P_{1560} is the peak power of 1560 nm beam at the beam waist of 780 nm, and $\omega_{0,780}$ and $\omega_{0,1560}$ are the respective beam waists of 780 and 1560 nm respectively, at the focal points of 780 and 1560 nm beam. $\omega_{z,1560}$ is the beam waist of 1560 nm beam at the focal point of 780 nm. Thus the effective intensities of 780 and 1560 nm beams at the focal point of 780 nm are found to be 1.46×10^{13} and 2.32×10^{10} Wm^{-2}. As a result, the total effective sum of intensities at the focal point of 780 nm is calculated as 1.46×10^{13} Wm^{-2}. Similarly, we calculated the peak intensity of 1560 nm (I_{1560}) at 1560 nm focal point as

$$I_{1560} = P_{1560} / \pi\omega_{0,1560}^2, \tag{6}$$

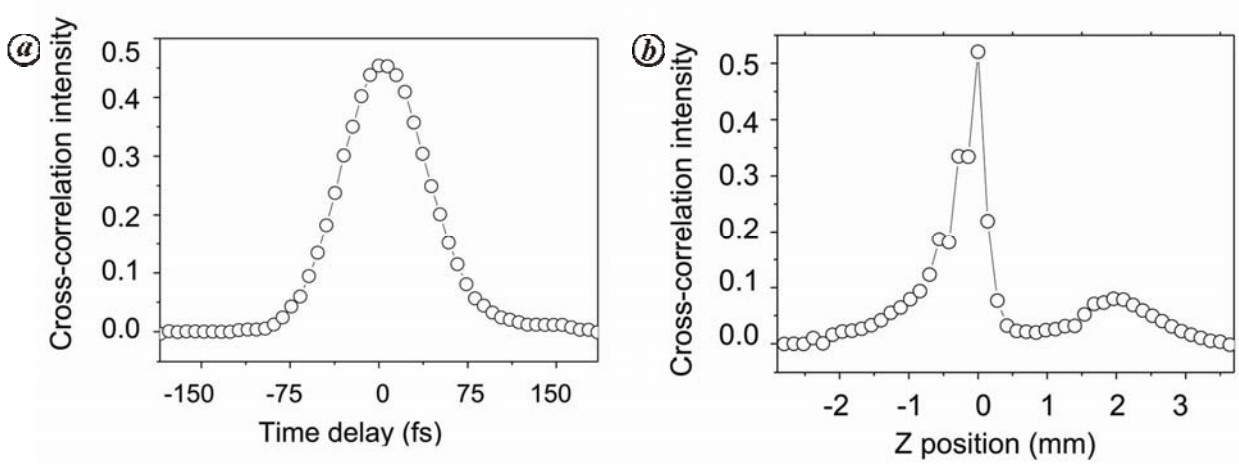

Figure 4. Cross-correlation trace recorded (***a***) on time axis when the BBO is at $Z = 0$ mm and (***b***) on Z axis at $t = 0$ fs.

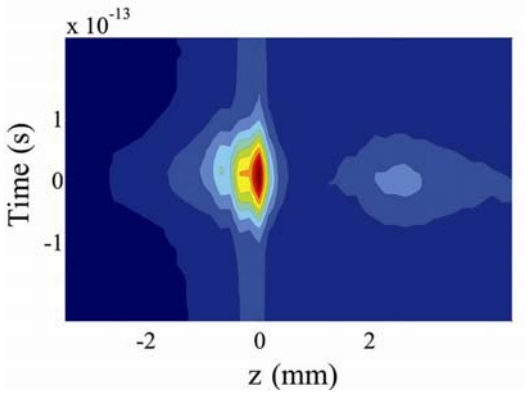

Figure 5. Representation of 2-D image of the cross-correlation signal recorded at each Z positions by moving the BBO across the focal point of the lens along the Z-axis.

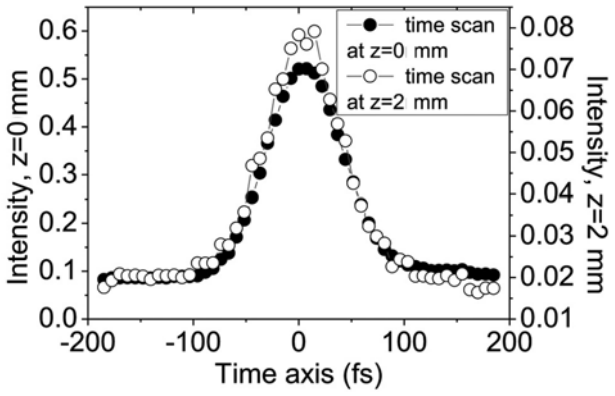

Figure 6. Cross-correlation traces at $Z = 0$ mm and $Z = 2$ mm.

where P_{1560} is the peak power of 1560 nm beam at the beam waist of 1560 nm and $\omega_{0,1560}$ is the beam waist of 1560 nm beam at the focal point of 1560 nm. We calculated the effective peak intensity of 780 nm (I_{780}) beam at the focal point of 1560 nm beam as

$$I_{1560} = \frac{P_{780}}{\pi\omega_{z,780}^2} \times \left[\frac{\omega_{0,780}}{\omega_{z,780}}\right]^2 \times \exp\left[-2\left(\frac{\omega_{0,1560}}{\omega_{z,780}}\right)^2\right], \qquad (7)$$

where P_{780} is the peak power of 780 nm beam at the beam waist of 1560 nm, $\omega_{0,780}$ and $\omega_{0,1560}$ are the respective beam waists of 780 and 1560 nm at their corresponding focal points. $\omega_{z,780}$ is the beam waist of 780 nm beam at the focal point of 1560 nm. Thus, the effective intensities of 780 and 1560 nm beams at the focal point of 1560 nm are found to be 6.88×10^9 and 2.24×10^{12} Wm^{-2}. Consequently, the total effective sum of intensities at 1560 nm focal point is calculated as 2.25×10^{12} Wm^{-2}. Thus the intensity ratio of SFG signals originating at $Z = 0$ mm and $Z = 2$ mm is calculated as 6.4. In the present experiment, the collinear SFG cross-correlation intensity at the focal point of 780 nm is 6.2 times higher as compared to that at 1560 nm focal point as is observed in Figures 4 *b* and 5 and correspondingly supports the value obtained from the calculation.

However, irrespective of the intensity difference, the characteristic widths of the cross-correlation traces are found identical as measured at the two wavelength dependent focal points (Figure 6) at $Z = 0$ mm and $Z = 2$ mm on the Z-axis. These characteristic widths also show good agreement with the width obtained from the XFROG (cross-frequency resolved optical gating) trace measured at 520 nm (Figure 7 *a*).

Variation in widths of cross-correlation traces recorded at different BBO positions on the Z axis (Figure 7 *b*) clearly shows two minima at $Z = 0$ mm and $Z = 2$ mm, which in turn, indicates that the shortest possible temporal correlations are only possible at two foci resulting from chromaticity of the focusing lens for two wavelengths. Thus, for collinear SFG intensity cross-correlation measurement using a single chromatic lens, we show that it is important to keep the NLO crystal exactly at one of the

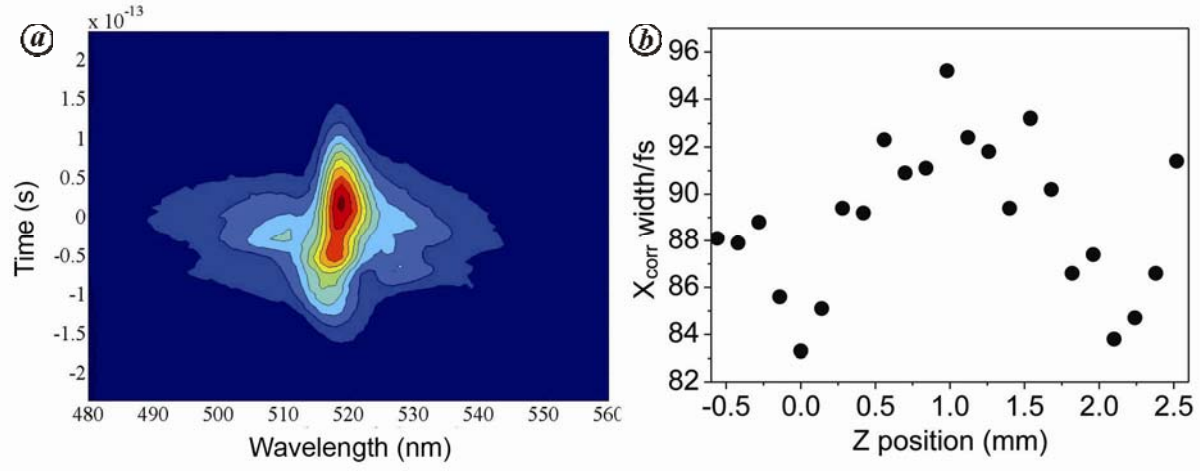

Figure 7. ***a***, XFROG trace collected at 520 nm and ***b***, variation of cross-correlation widths as measured at different BBO positions on the *Z*-axis.

two foci of the lens to get the correct cross-correlation width, otherwise the measured pulse width is higher than the actual width. Since the correlating beams are collinearly interacting inside the BBO crystal, the characteristic width of the SFG cross-correlation mostly depends on the position of the crystal on the *Z*-axis rather than other factors, such as crystal orientation, individual beam spot sizes, etc.

We generated two-dimensional (2D) image of second-order nonlinear SFG process at 520 nm in a nonlinear BBO crystal by using two collinear femtosecond laser pulses at 1560 and 780 nm. Scanning the BBO crystal across focal point of a lens, SFG cross-correlation signals were measured at each individual BBO positions on the *Z* axis and their corresponding plot created a 2D image of the second order process. Chromaticity of the lens results in two different SFG maxima corresponding to the two wavelength-dependent focal spots, which match the shortest possible temporal correlation. Analysis of the 2D image suggests that though signal intensity depends on factors like crystal orientation, individual beam spot sizes, etc., characteristic width of the SFG signal is distinctive of the position of BBO crystal with respect to individual focal points of laser beams used. As long as the NLO crystal is kept at any one of the two foci on *Z*-axis, the characteristic SFG width and the shortest possible temporal correlation remain unaltered; thus highlighting the spatiotemporal aspect of the experiment.

1. Boyd, R. W., *Nonlinear Optics*, Academic Press, San Diego, 2003.
2. Romero, C., Aldana, J. R. V., de Méndez, C. and Roso, L., Non-collinear sum frequency generation of femtosecond pulses in a micro-structured β-BaB_2O_4 crystal. *Opt. Exp*., 2008, **16**, 18109–18117.
3. Karthick Kumar, S. K., Goswami, T., Bhattacharyya, I. and Goswami, D., Visible 20-femtosecond pulse generation by double-pass non-collinear optical parametric amplifier (NOPA). *Curr. Sci*., 2009, **96**, 1496–1500.
4. Bhattacharyya, I., Dutta, A., Ashtekar, S., Maurya, S. K. and Goswami, D., Decoding coherent information in femtosecond shaped laser pulses. *Curr. Sci*., 2010, **99**, 476–484.
5. Fittinghoff, D. N., Squier, J. A., Barty, C. P. J., Sweetser, J. N., Trebino, R. and Muller, M., Collinear type II second-harmonic-generation frequency-resolved optical gating for use with high-numerical-aperture objectives. *Opt. Lett*., 1998, **23**, 1046–1048.
6. Fittinghoff, D. N., Millard, A. C., Squier, J. A. and Muller, M., Frequency-resolved optical gating measurement of ultrashort pulses passing through a high numerical aperture objective. *IEEE J. Quant. Electron*., 1999, **35**, 479–486.
7. Krylov, V., Gallus, J., Wild, U. P., Kalintsev, A. and Rebane, A., Femtosecond noncollinear and collinear parametric generation and amplification in BBO crystal. *Appl. Phys. B*., 2000, **70**, 163–168.
8. Amat-Roldán, I., Cormack, I. G. and Loza-Alvarez, P., Ultrashort pulse characterisation with SHG collinear-FROG. *Opt. Exp*., 2004, **12**, 1169–1178.
9. Sheik-Bahae, M., Said, A. A. and Van Stryland, E. W., High-sensitivity, single-beam $n(2)$ measurements 1989 High-sensitivity, single-beam $n(2)$ measurements. *Opt. Lett*., 1989, **14**, 955–957.
10. Sheik-Bahae, M., Said, A. A., Wei, T.-H., Hagan, D. J. and Van Stryland, E. W. Sensitive measurement of optical nonlinearities using a single beam. *IEEE J. Quant. Electron*., 1990, **26**, 760–769.
11. Goswami, D., High sensitive measurements of absorption coefficient and optical nonlinearities. *Opt. Commun*., 2006, **261**, 158–162.
12. Sharan, A., Hosseini, S. A. and Goswami, D., Single experimental setup for high sensitive absorption coefficient and optical nonlinearities measurements. In *Lasers and Electro-Optics at the Cutting Edge* (ed. Larkin, S. B.), Nova Publishers, NY, 2006, pp. 43–61.

ACKNOWLEDGEMENTS. D.G. thanks the funding support of MHRD and ISRO-Space Technology Cell, Govt of India. I.B. thanks the Institute Post-Doctoral Fellowship from the Department of Chemistry, IIT Kanpur. We also thank Mrs S. Goswami for language correction and editing.

Received 29 February 2016; accepted 10 September 2016

doi: 10.18520/cs/v112/i04/830-834